UNIVERSITY OF GRONINGEN

FACULTY OF MATHEMATICS AND NATURAL SCIENCIES

KAPTEYN INSTITUTE

BACHELOR'S THESIS

Looking for sulfur in the Sculptor dwarf spheroidal galaxy

Author:
Michael ZURAVLOVS

Supervisor:
Prof. Eline TOLSTOY

A thesis submitted in fulfillment of the requirements for the degree of Bachelor of Astrophysics

in the

Kapteyn Astronomical Institute

August 23, 2016

UNIVERSITY OF GRONINGEN

Abstract

Faculty of Mathematics and Natural Sciences
Kapteyn Astronomical Institute

Bachelor of Astrophysics

Looking for sulfur in the Sculptor dwarf spheroidal galaxy

by Michael ZURAVLOVS

Sulfur is a poorly studied element in individual red giant branch stars outside the Milky Way. It has been shown to behave like other α-elements in this Galactic Halo of red giant branch stars. High-resolution ESO VLT/FLAMES/UVES spectra was used to look for the S I triplet at 9213, 9228, and 9238 Å for 8 individual stars in the Sculptor dSph. This involved significant data reduction, namely sky removal, telluric corrections, heliocentric corrections and co-adding same stars spectra. However, convincing evidence of the presence of sulfur in the stars was not found.

Chapter 1

Introduction

We are living on the Planet Earth. Our planet is turning around a star that we call the Sun. Sun is the central object of our solar system. Among 200 billion stars in our Milky Way galaxy, our solar system is not the only one. Despite this fact, it is impossible to see any of their solar systems with a naked eye. Behind the Milky Way a great amount of different types of galaxies exist: spirals, ellipticals, irregulars, where each of them has their own brightness, size, mass, opacity, velocity, age. No two galaxies are the same. The main topic of interest in this project is a Dwarf Spheroidal Galaxy (dSph).

dSphs are one of the simplest galaxies that are known of presently. Spectra of individual dSph red giant branch (RGB) stars can be studied and metal content can be determined that gives the information on the chemical evolution that in turn provides the understanding of a galactic formation and evolution. Typically, dSphs has very metal-poor stars and a unique ability of loosing gas instead of attracting it (Mateo, 1998), thus the amount of HI gas is negligible. Also, dSphs characterize a roughly spheroidal shape and contain old stars in it. Usually, these galaxies are found in the vicinity of large galaxies, such as ours.

Nearby galaxies like dSph can be studied star by star, which belong to the Local Group (Figure 1.1) that is a group of galaxies that covers a diameter about 2 Mpc. Milky Way and Andromeda are the most massive galaxies in the Local Group. Since the majority of galaxies, that are not just in the Local Group but in the whole Universe, are Dwarf Galaxies, there is a great interest in examining them in detail (McConnachie, 2012). The number of stars in a dSph could be calculated to be around 4 million. This number is very small in comparison with the number of stars in galaxies such as the Milky way. At greater distances individual stars cannot be observed and especially high resolution spectra cannot be taken. dSphs are being examined in the Local Group, a good laboratory for astronomers.

The interest in dSphs has raised after the pioneer work of (Aaronson, 1983). In the same year, in a theoretical work of (Faber, 1983), a large amount of non-luminous matter from individual RGB stars in the dSphs, due to the high mass-to-light ratio (even higher than in globular clusters) was discussed. Measurements of metallic abundances were done by (Shetrone, 2001; Shetrone, 2003; Geisler, 2001). Chemical evolution of the dSphs has not been affected by very massive stars judging by α-element abundance (Tolstoy, 2003).

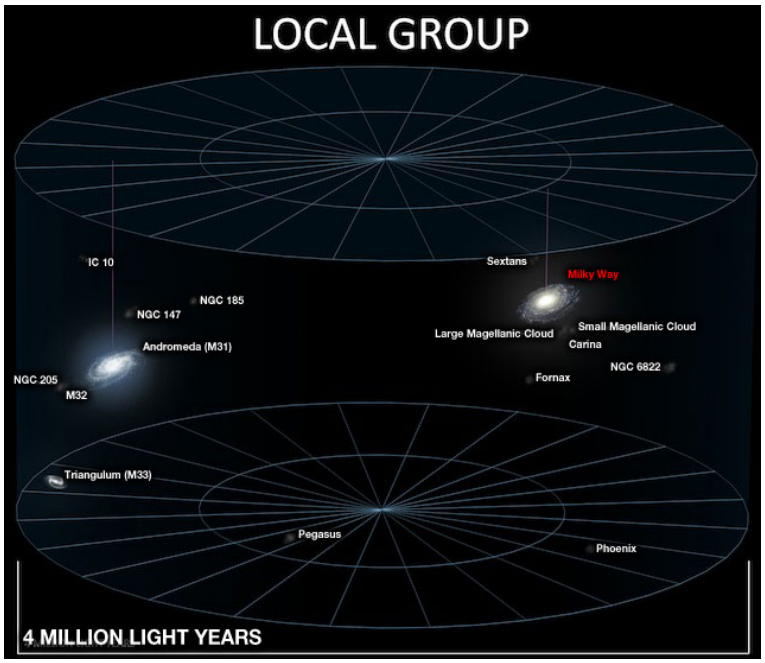

FIGURE 1.1: The approximate observed locations and sizes of a few galaxies in the Local Group. Milky way is on the right; Andromeda is on the left. It is just a representation of the scale of the Local Group. Image from (Hammonds, 2013).

CMDs constructed from dSph's stars were analyzed that led to the conclusion that dSphs are composed of composite stellar populations. Examination of different stars in the RGB have shown that dSphs have internal metallicity dispersion (Suntzeff, 1993; Smecker-Hane, 1999). More precise information about stars metallicity can be found by analyzing stars high-resolution spectra. But first, it is important to consider the possible origin of dSphs stars.

A cold gas cloud that overcomes, the so called, Jeans limit, collapses into a star, where all the chemical elements in the Universe that are heavier than lithium are being created. In some time, "metals" (elements heavier than He) are dispersed into the stars surroundings, mostly due to energetic supernovae explosions and stellar winds. It is known, that Type II supernovae mostly produce so-called α-elements (O, Ca, Mg, S, Si and Ti), whereas Type Ia supernovae synthesize Fe group (Fe, Co, Ni and Zn). Thus, a new generation of stars with a fraction of metals that increases with time are formed from enriched gas. Since photospheres retain the most chemical composition of the stars birth environment, spectral analysis (star's spectrum is a spectrum of its photosphere) can give a clue about the chemical enrichment history of the stars and systems they are in.

One remarkable tool, that efficiently obtains spectra is a multi-object high resolution (HR) spectrograph FLAMES/UVES of the ESO Very Large Telescope (VLT) in Chile (Pasquini, 2002). FLAMES/UVES has resolution

of about 40,000. The spectrograph can cover from 3000 to 11000 Å, however it can cover a few thousand Ångström per spectrum. Such an instrument can collect a useful data that can be reduced by an automatic pipeline, that simplifies the reduction process.

The first results on stars in dSph from the UVES spectrograph were obtained during the commissioning of the instrument in the 2000 (Bonifacio, 2000). After this more studies were published, but with a low number of stars probed (Shetrone, 2003; Bonifacio, 2004; Geisler, 2005). It is worth mentioning that not only UVES instrument was used for dSph observations, but also the Keck I telescope and the High Resolution Echelle Spectrometer (HIRES) were involved in the observations of dSph galaxies (Shetrone, 2001). It was problematic to observe faint dSphs stars because to get conclusive data, up to 5 hours of exposure time per star is required. The problem with low number of observations was solved when HR spectrographs with multiplex capabilities come in sight (FLAMES multi-fiber facility for UVES (Pasquini, 2002)). Larger samples of stars measured in the same period of time boosted the productivity (Monaco, 2005; Sbordone, 2007; Monaco, 2007; Letarte, 2007; Skuladottir, 2016).

In this thesis the data from the Sculptor dSph galaxy collected by the FLAMES/UVES was used.

1.1 The Sculptor dSph galaxy

The dSph galaxy studied here is the Sculptor dSph. This well studied low surface brightness galaxy is located in the constellation of Sculptor relatively close by, in the Local Group. The Sculptor dSph is located at high Galactic latitude b = -83° and longitude l=287.5° (Figure 1.2). The discovery of the galaxy was made by (Shapley, 1938). Despite the fact that the galaxy was discovered almost a century ago, new technological advances and improvements regarding the resolution of observations help to discover more and more stars, and analyze them.

The basic properties of the dSph Sculptor galaxy are summarized in Table 1.1, data was taken from the NASA/IPAC Extragalactic Database. A picture of the Sculptor dSph in optical that was obtained from SIMBAD database is shown on Figure 1.3, in fact, even if a collective structure of stars is hardly seen, this constellation of stars is the Sculptor dSph since these stars have a measurable bound.

Since the dSph Sculptor galaxy is close enough to us it is possible to observe the brightest individual stars, infer their magnitudes and create CMDs. The first studies of star formation history (SFH) of the galaxy has been carried by using CMD. The first interpretations after analyzing first CMDs by observing the RGB stars of the dSph Sculptor galaxy has led to the interpretation that the galaxy has small star formation, mainly old, but with main-sequence turn-off stars as young as 5 Gyr (Da Costa, 1984). The photometric analysis of the Sculptor galaxy taken with the Hubble Space Telescope WFPC2 tells us that the absence of faint stars V=21 mag. rules out

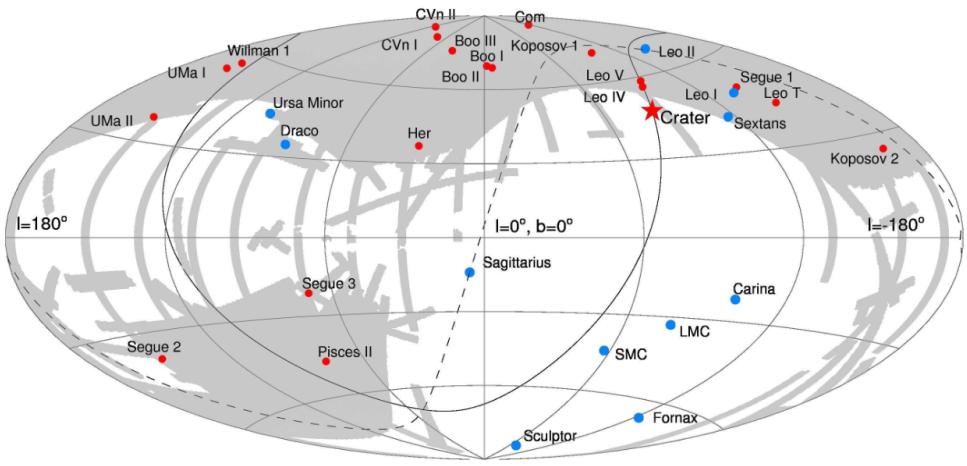

FIGURE 1.2: Milky Way's dwarf galaxy satellites in Galactic coordinates. Blue circles are classical dwarf galaxies, and red circles are the SDSS ultra-faint satellites. The imaging footprint of SDSS DR8 is shown in grey. The Sculptor dSph at longitude l=287.5° and latitude b = -83°. From Belokurov et al. (2014).

TABLE 1.1: Properties of the Sculptor dSph (NASA/IPAC Extragalactic Database). Mass and mass-to-light ratio are taken from (Battaglia, 2013). Distance is taken from (Pietrzyński, 2008).

Property	**Value**
Radial velocity (km/s)	110 ± 1
Major Diameter (arcmin)	39.8
Absolute magnitude and filter	-10.97 $\pm$ 0.51 V
Mass (inside 1.8 kpc)($M_{\odot}$)	$3.4 \pm 0.7 \cdot 10^8$
Mass-to-light ratio (inside 1.8 kpc)((M/L)$\odot$)	158 ± 33
Distance (kpc)	86 ± 5

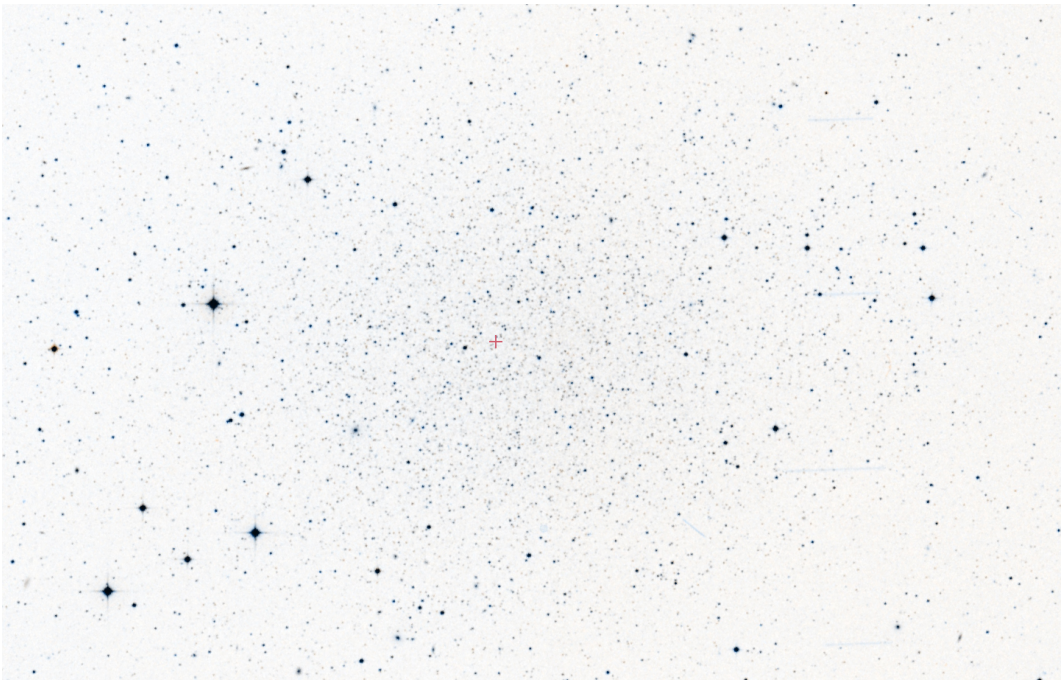

FIGURE 1.3: The Sculptor dSph galaxy negative picture in optical was taken from SIMBAD database by Aladin Lite software. A red cross is the center of the galaxy. Angular size is 25.7 arcmin.

the possibility of star formation more recent than 2 Gyr ago (Monkiewicz, 1999).

The star formation history (SFH) was qualitatively determined by the work of (Boer, 2012). Figure 1.4 shows star formation rate (SFR) at each age of the galaxy and the metallicity distribution function (MDF) for a number of stars. Turns out that the Sculptor dSph is not experiencing any significant star formation for about 6 Gyr from now. But before, between 14 and 7 Gyr ago 7.8×10^6 $M_\odot$ was formed within a radius of 1.5 kpc. The most metal-rich, young galactic stars are more centrally concentrated, while metal-poor stars are present at all radii. Most of the galaxy stars have metallicities [Fe/H] equal to -2 +/- 0.5 dex. It means that the metallic content of these stars is much less than in the Sun and stars are much older. Thus, the Sculptor dSph could be very helpful in studying ancient stellar populations.

Dwarf Abundance and Radial-velocity Team (DART) (Tolstoy, 2006) made a good progress towards understanding that the kinematic and evolutionary processes of the Sculptor dSph are not as simple as it was thought and the Sculptor dSph is not a "building block" of the largest galaxies in the Local Group. The galaxy kinematics has been well studied on a sample of 470 stars from low resolution spectra (R-6500) (Battaglia, 2008). Over more than 15 years DART has been presenting results of abundances of different elements in the galaxy. The latest work of (Skuladottir, 2016) was dedicated to sulfur, zinc and carbon abundances measurement; this work was also the first comprehensive study of the sulfur abundances in the galaxy. The main

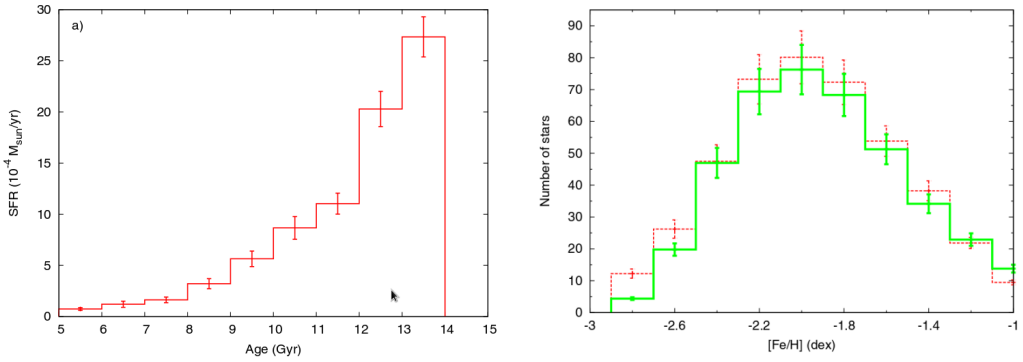

FIGURE 1.4: Left graph: Star formation history of the Sculptor dSph galaxy. Right graph: The best matching simulated MDF (green) solid histogram and observed MDF (red) histogram from spectroscopic observations. From (Boer, 2012).

TABLE 1.2: Overall number of observations of each star in different wavelength ranges.

Star	**4770 - 5800 Å**	**5820-6830 Å**	**6730-8540 Å**	**8650-10420 Å**
UET0248	8	8	10	10
Ut125	2	2	10	10
UET0235	5	5	10	10
UXET0324	8	8	10	10
UET0381	8	8	10	10
UET0360	8	8	10	10
UET0409	8	8	10	10
UCET0136	6	6	0	0

goal of this thesis is to expand Asa's work by looking for an abundance of sulfur in different stars.

In total 36 different observations in different bands (4770, 5820, 6730, 8650 Å) in the period between 2012-07-15 and 2013-11-18 were obtained. 8 different bright and relatively cool RGB stars from the Sculptor dSph galaxy were observed and analyzed. These 8 stars were chosen randomly except the Ut125 star, since this is a telluric star (very bright source star). Random selection of RGB stars is a good choice for obtaining valid sampling of the whole population. Repetitive observation of the same stars were made, since it helps to get rid of bad pixels, distinguish cosmic rays, tackle very noisy data and achieve more accurate results. Number of observations of each star in different wavelengths are summarized in the Table 1.2. Note that I was provided with the stars data that was already pipeline processed and I did not make observations by using VLT on my own.

The importance of having accurate stars data ensures qualitative and fruitful data analysis. In spectroscopic analysis lines may or may not be found. It can give ideas about the evolution of the stars and their origin.

Also, knowing the origin of the Local Group galaxy stars, the evolution of Milky Way could be determined.

1.2 Sulfur

Sulfur is an α-element, means that it is one of the most abundant isotopes that is made out of the He-nuclei. Sulfur is one of the most challenging element among all α-elements in the Local Group to study and the very first survey of sulfur abundances in individual stars in dSph was made by (Skuladottir, 2016). Previously, sulfur abundances were examined only within the Milky Way. The paper of (Jenkins, 2009) tells that sulfur most likely is not bound onto interstellar dust, therefore, sulfur abundances in stars could be compared to measurements in ISM, like damped Lyman-α absorption systems. It is more interesting to inspect the element more attentively.

The first clues of α-element scarcity in dSph galaxies compared to the Milky Way halo or disc was recorded by (Shetrone, 1998; Shetrone, 2001; Tolstoy, 2003; Tolstoy, 2009). At low [Fe/H], the ratio [α/Fe] is the same in each galaxy (Figure 1.5). As [Fe/H] starts to increase, the ratio [α/Fe] in dSphs evolves down to lower values.

The star-formation timescale in a system is traced by [α/Fe]. Super Novae Type II (SNe II) that occur after the explosion of massive stars in 10^7 yr after formation is believed to be the most important production site for the α-elements like Si, Ca, S and Ti. The ratio of Type II Supernovae massive stars to Type Ia supernovae intermediate mass binary systems with mass transfer (SNIa) change [α/Fe]. This is because SNI live longer than SNII and as soon as they start to contribute they dominate the iron enrichment and [α/Fe] decreases.

α-elements can easily be measured in Red Giant Branch (RGB) stars selected from a CMD. However, there are contraries in different studies that question whether sulfur is a typical α-element. Some studies find no correlation between [S/Fe] and [Fe/H], whilst others found an increase of [S/Fe] towards lower [Fe/H] (Takeda, 2011). All contraries were summed up in the work of (Ryde, 2014). From the same work [S/Fe] vs. [Fe/H] values were demonstrated on the Figure 1.6, where the results from different papers were collected. Judging by the blue line (Kobayashi, 2011), at low metallicities [S/Fe] values doesn't change gradually. At higher metallicities [Fe/H]>1 values of [S/Fe] decrease more steeply with the increase of [Fe/H], such a trend can be caused by the yields from SNe Type I.

Usually, Local Thermodynamic Equilibrium (LTE) is assumed when stellar abundances are analyzed, but sulfur is sensitive to the deviations from LTE. Thus, non-LTE corrections need to be taken into account (Takeda, 2005). LTE assumption is valid for S I 8683, 8694 Å lines, when for commonly used S I lines of multiplet 1, namely 9212, 9228, 9237 Å non-LTE effect need to be assumed. Also, multiplet 1 lines are located in the region covered with telluric absorption lines, which need to be removed before the

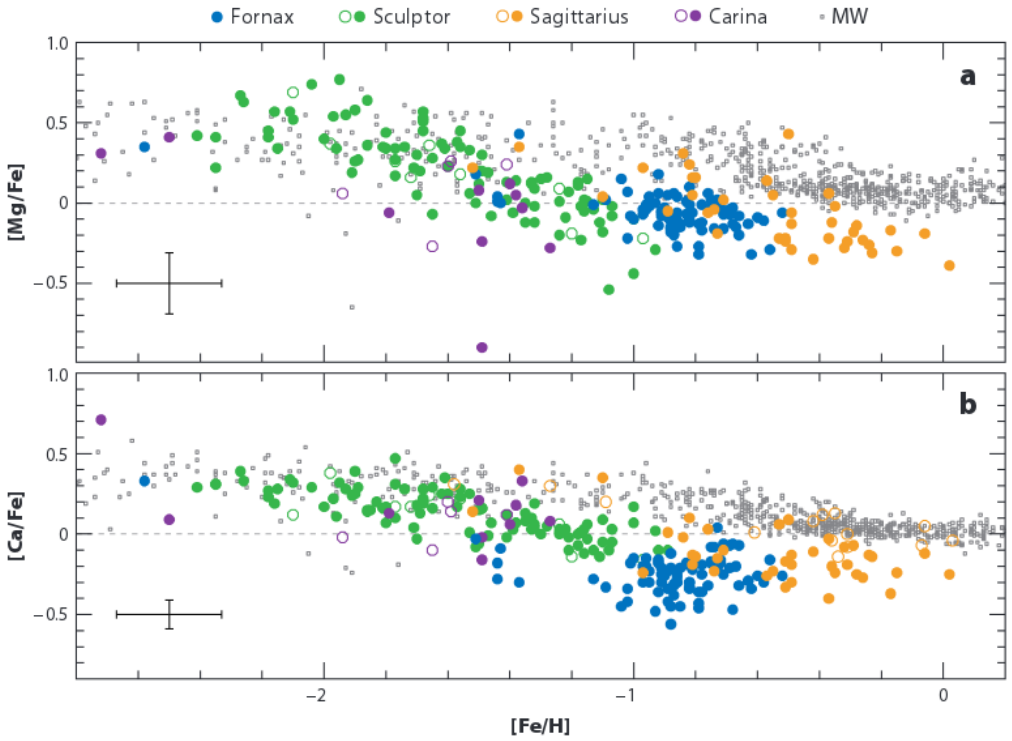

FIGURE 1.5: α-element abundance ratios of RGB stars in four nearby dwarf spheroidal galaxies (coloured dots) and the Milky Way (grey dots). From (Tolstoy, 2009)

spectra can be analyzed.

So, the key moment in measuring Sulfur lines is that a hint could be found towards exploring the chemical enrichment history.

1.3 This Thesis

HR spectra of 8 individual RGB stars from the Sculptor dSph observed by FLAMES/UVES was used. Cleaning of the stars spectra was done, namely, sky was removed, telluric lines were removed in the region where sulfur lines from S I triplet could be found (9000-9500 Å), heliocentric velocity corrections were made and the different spectral time datas from the same stars were combined. In the end, sulfur line regions on the spectrum of each star were inspected for extending the knowledge of chemical enrichment history of the Sculptor galaxy. All the technical part was done in Python and IRAF.

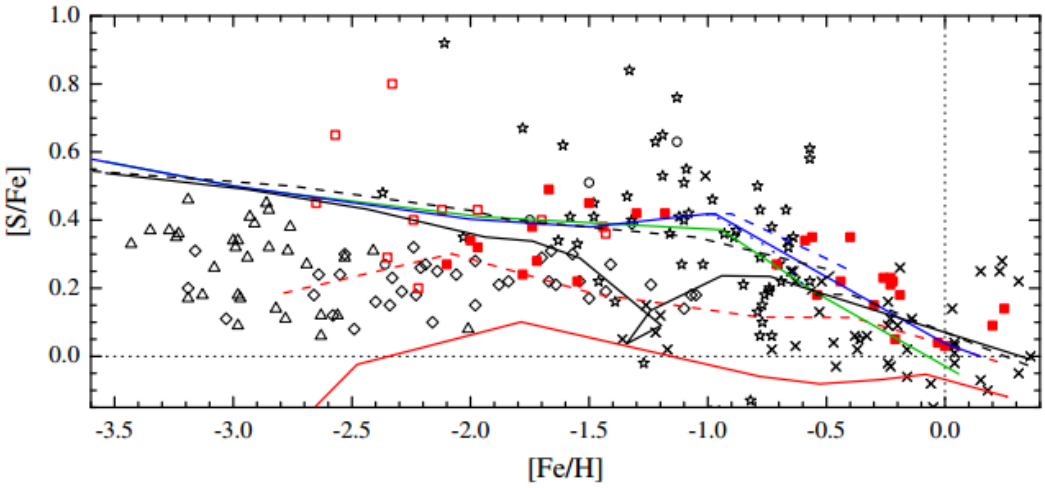

FIGURE 1.6: Taken from (Matrozis, 2013) that was reproduced by (Ryde, 2014) by adding the data (solid and open red squares). Crosses are from (Takada-Hidai, 2002), stars are from (Caffau, 2005), rhombi are from (Nissen, 2007), circles are from (Caffau, 2010), triangles are from (Spite, 2011). Blue dotted, solid and dashed lines are models from (Kobayashi, 2011), the red solid line (Timmes, 1995) and red dashed line shows the model where iron yields are reduced by a factor of two, the green line is prediction of (Kobayashi, 2006) for the solar neighborhood, dashed and black lines are from (Brusadin, 2013) double-infall model with and without outflow, respectively.

Chapter 2

Sky removal

2.1 Introduction

Observing an astronomical object's spectra is not enough to analyze it straight away. Usually, there are some disturbing factors that should be taken into account and can't be avoided. One of these factors is a sky light. It is a light that comes from everywhere, but not from the star. The light comes from natural light sources in the night sky including moonlight (especially when the Moon is above the horizon), starlight, and airglow. The dependency of the emission features in the sky spectrum on the sunspot cycle was first pointed out by (Rayleigh, 1928). Also, light from distant galaxies, interstellar medium, cosmic microwave background (CMB) and ambient city light contributes to the sky. The factors depend greatly on time and location, and sky can vary more than on one magnitude (Patat, 2008).

The solar ultraviolet radiation ionizes the upper Earth's atmosphere atomic and molecular components, which induce the airglow line and continuum emission that dominate near-UV, optical and near-IR sky emission (Khomich, 2008). Much weaker, but not less important due to it's constant presence, the component is scattered starlight (Mattila, 1980; Leinert, 1998). A zodiacal light (solar radiation reflecting off interplanetary dust grains mainly distributed in the inner solar system) is a significant component at optical wavelengths (Levasseur-Regourd and Dumont, 1980; Leinert, 1998). The extinction of radiation from astronomical objects by Rayleigh scattering off of air molecules and Mie scattering off of aerosols (they are wavelength dependent) was characterized at different telescope sites (Gutiérrez-Moreno, 1982; Gutiérrez-Moreno, 1986; Patat, 2011). All these sky components are shown in Figure 2.1.

Sky can be removed from a star's spectra in a few ways, but the most important one is when sky lines should go away and S/N needs to improve or at least not decrease. The simplest way is to measure a spectrum of the closest region to the object of interest, where brightness is the least. This is the sky spectrum. Best, if the sky and the object spectra are measured in the same time. Then, the sky spectrum can be subtracted from the object spectrum. The example of a measured star spectrum, sky spectrum and its good removal is shown on Figure 2.2

However, as was mentioned in Chapter 1, VLT's FLAMES/UVES has 8 fibers that measure separate objects in the same time. So, for convenience each observation provides different stars data from 7 fibers and a sky data

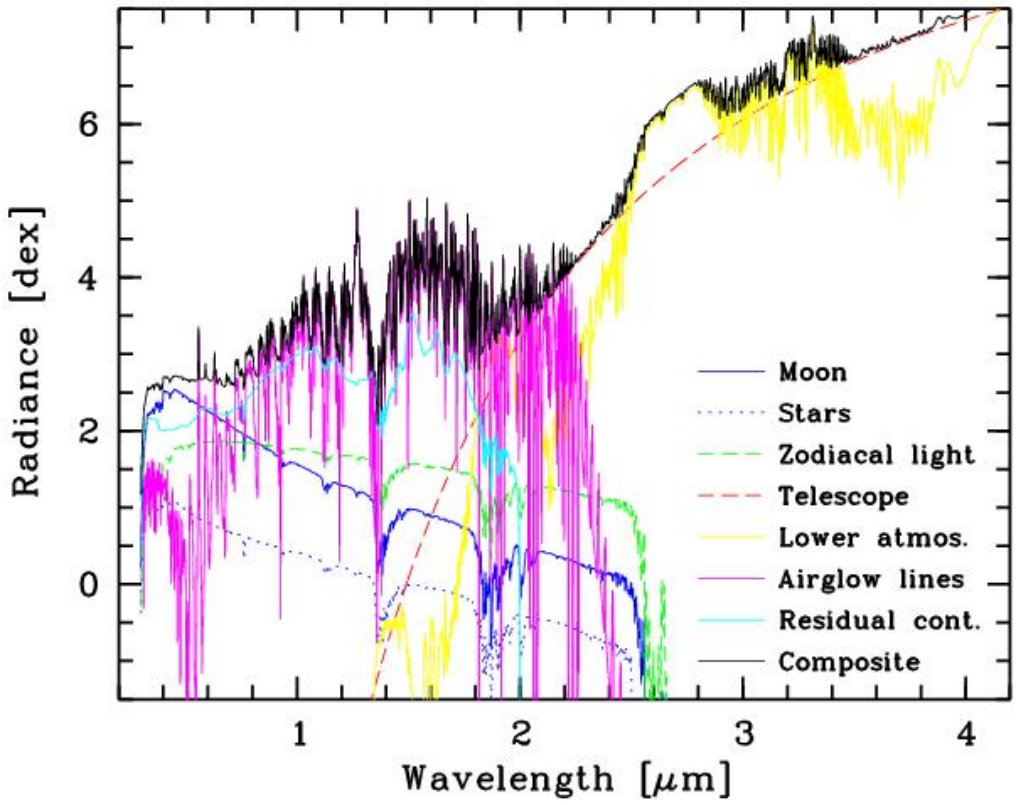

FIGURE 2.1: Components of the sky model in logarithmic radiance units for wavelengths between 0.3 and 4.2 μm. This example, with the Moon above the horizon, shows scattered moonlight, scattered starlight, zodiacal light, thermal emission by the telescope and instrument, molecular emission of the lower atmosphere, airglow emission lines of the upper atmosphere, and airglow/residual continuum. From (Noll, 2012).

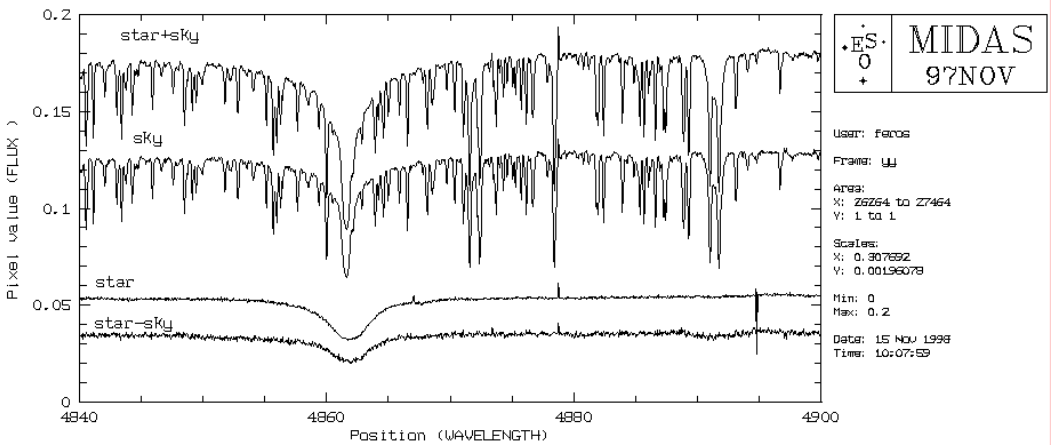

FIGURE 2.2: Example of a sky removal from a spectrum. With a star+sky and sky data given, star data can be obtained. Taken from https://www.lsw.uni-heidelberg.de/projects/instrumentation/Feros/Installation.html.

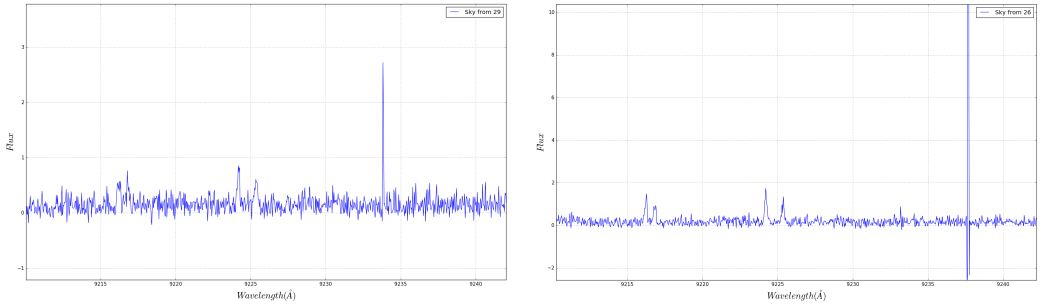

FIGURE 2.3: Sky region between 9210 and 9242 Å obtained by VLT FLAMES/UVES. Peaks are cosmic rays.

from one fiber; an example of a data is shown on a Figure 2.3. Hence, 2 different ways of the sky subtraction could be done:

- median of all sky data (total 36) can be obtained and subtracted from the every single object data
- single sky data can be subtracted from the objects data within the framework of each observation.

Second sky reduction method was used in this work, because the obtained spectra were taken over a long time frame and the night-to-night variations are quite strong.

If we take a close look at Figure 2.3 high peaks can be noticed. These peaks are not intrinsic for the dSph stars spectra or sky spectra, and in each data set these peaks occur randomly in different places. These are cosmic rays (CR). If the sky with a CR in the spectra will be subtracted from the stars spectra an unwelcome and non-existent absorption line would be added to the data spectra. To avoid this, CR needed to be removed from each sky spectra.

A Python code was written to remove CRs and the sky.

2.2 Results

First of all, each sky spectrum was checked. It was noted that for different observation bands sky intensities are different. In the red band CR have lower values in comparison with the blue band.

CR was removed from a sky spectra as follows. CR were found in the spectra and the median of 40 pixels (less than 1 Å) around the CR were computed. Such a number of pixels were chosen because a good median value can be computed from this sample and some CRs are wider than others (better to have some spare pixels to remove CRs definitely). Then the pixels with CR were changed with computed median values Figure 2.4.

When CR were removed from sky spectra, one more procedure was made before removing sky from stars spectra. Since sky spectra are too

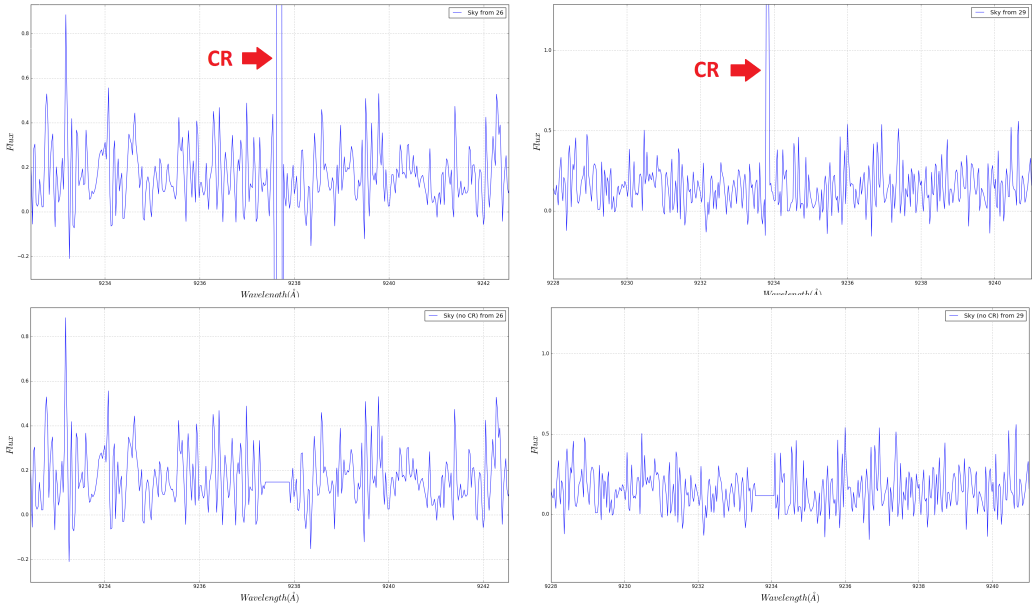

FIGURE 2.4: Two different sky spectra on the top have CR in the region between 9210 and 9242 Å. On the bottom spectra CR are removed by taking the median around them.

noisy having low signal-to-noise there is a risk of adding an excess noise to the stars spectra. Therefore, sky spectra need to be smoothed. The sky emission lines were kept in sky spectra after normalizing and smoothing it as these peaks are also found in star spectra and they are part of the sky spectrum.

After taking CR into consideration normalizing and smoothing the sky spectra, the sky were subtracted from the normalized stellar spectra (Figure 2.5a, 2.5b, 2.6a, 2.6b).

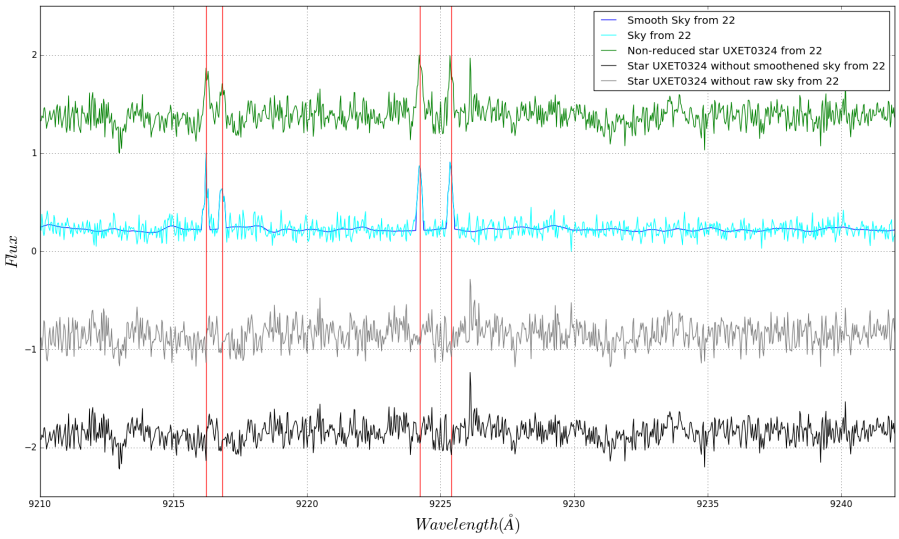

(A)

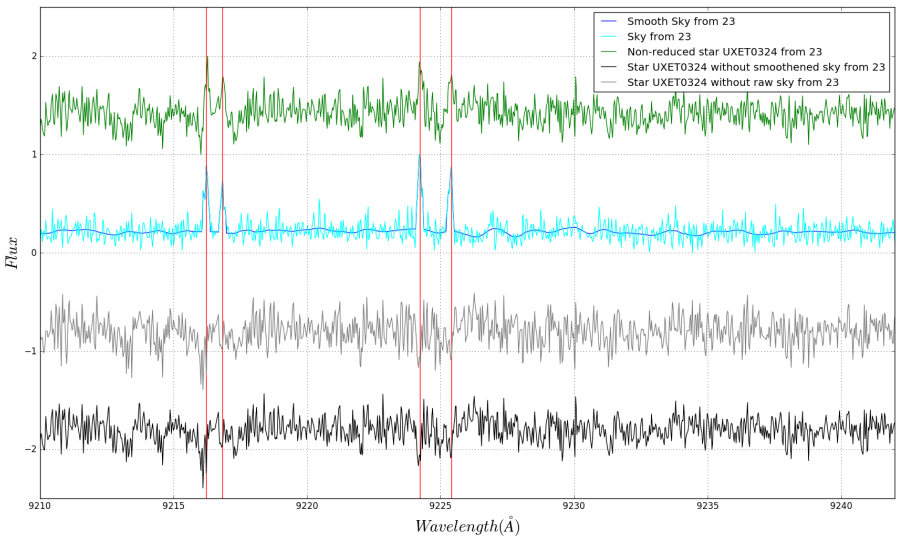

(B)

FIGURE 2.5: Resulting star spectrum (black) after smoothed sky spectrum with sky emission lines (blue) removal from the raw star spectrum (green). In comparison, star spectrum reduced from non-smoothed sky spectrum is more noisy (gray). Red lines are the sky emission lines positions. All lines are artificially shifted on y-axis for convenience sake.

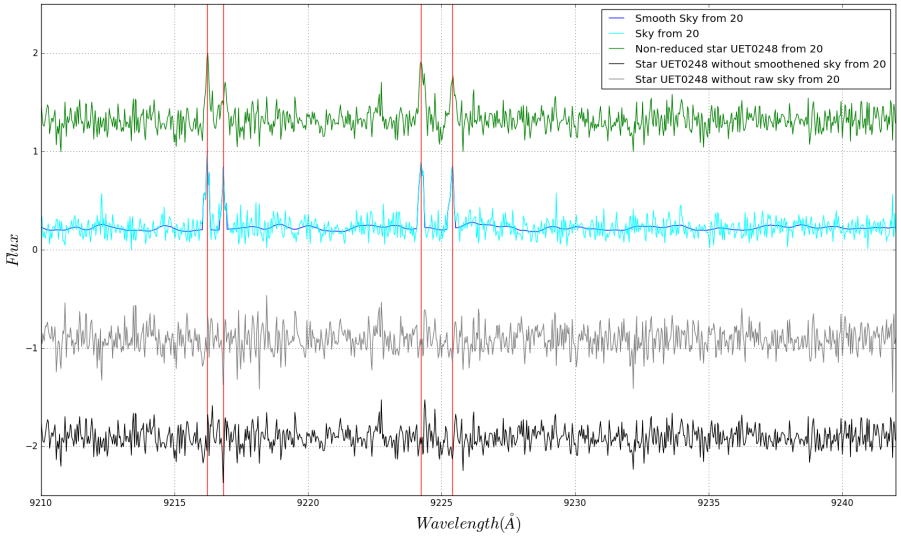

(A)

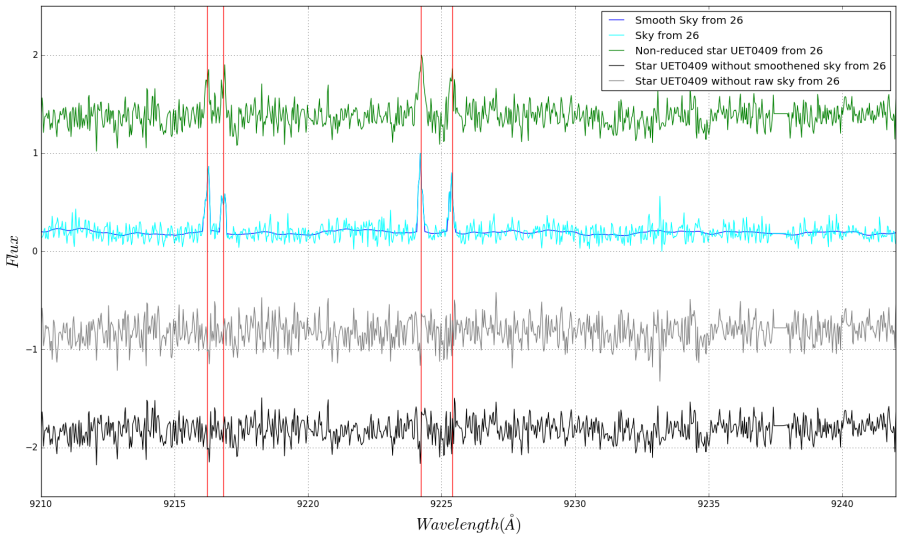

(B)

FIGURE 2.6: Similarly as at Figure 2.5a, 2.5b.

Chapter 3

Telluric's and heliocentric velocities

3.1 What are Telluric's

Ground-based astronomical spectroscopy has to face troubles related to the earth's atmosphere. Any light coming from an astronomical object passes through the Earth's atmosphere before it is detected by a telescope. Some of the frequencies of radiation (especially in the near-infrared) are absorbed by the Earth's atmosphere and molecules. Collectively they emit their own radiation. This atmospheric absorption lines are known as telluric lines.

In the red and near-IR region telluric lines are mainly the result of absorption by the ozone (O_3), oxygen (O_2), and water vapor (H_2O) (Adelman, 2002). Other telluric lines include Carbon dioxide (CO_2), methane (CH_4), nitrous oxide (N_2O) (Seifahrt, 2010) and sodium-D lines (Lundstrom, 1991). Among all different absorption lines H_2O is the most unpredictable and variable line. It was found that H_2O line does notably vary within a year (Lundstrom, 1991), but it is still hard to predict the line variation on the smaller time scale. Hence, telluric spectrum is not identical in different regions and at different times. Thus, the driest place with the lowest air-mass (high altitudes) for ground-based telescopes is required to minimize contamination of data by telluric lines and simplify the telluric reduction.

Telluric lines can be modeled by Doppler profile, Lorentz profile or by a combination of the two; a Voigt profile. A Doppler profile models a distribution of velocities of the atoms and molecules that cause the Doppler effect and the spectral lines broadening. Doppler broadening becomes dominant in the upper atmosphere, where the pressure is low. A Lorentz profile models collisions between atoms and molecules that causes pressure broadening. Pressure broadening becomes dominant in the lower atmosphere, where pressure is high. At the altitudes between 20 and 50 km Voigt profile is used. The example of synthetic telluric spectrum (taken from TAPAS) (Bertaux, 2014) is shown on Figure 3.1.

3.2 Telluric's removing method

Sometimes, telluric lines are not touched in the spectra because the regions of interest could not be contaminated by them. In our case telluric lines removal can't be skipped, because our main region of interest is S I triplet

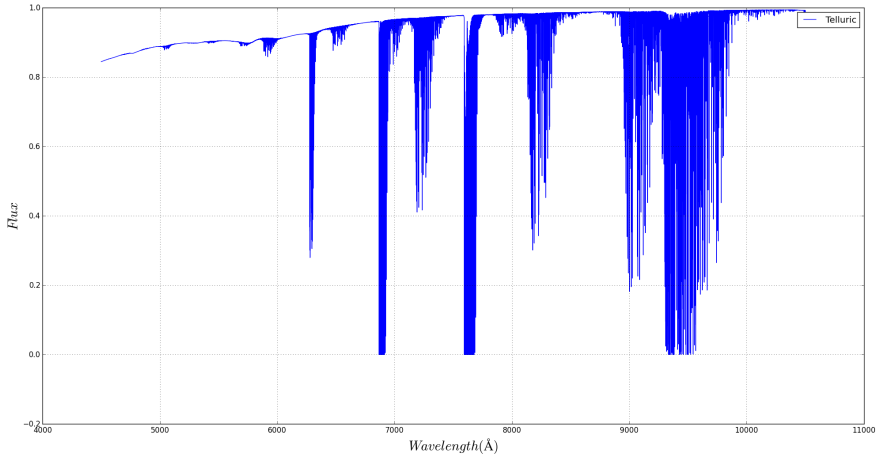

FIGURE 3.1: Normalized telluric spectrum taken from TAPAS (Bertaux, 2014) for a region 4500-10500 Å. If flux values are at 1 it means that no radiation is absorbed by the atmosphere, if flux values are at 0 - all radiation is absorbed by the atmosphere in this region.

region and it is full of telluric lines.

(Honeycutt, 1977; McCord, 1979; Cochran, 1981) has presented methods in which the telluric bands were treated as if they contained a linear term and a constant. After the removal of the linear component, the remaining parts were thought as if they were instrumental noise. Alternatively, in search of the atmospheric extinction in the near infrared (Manduca, 1979) used IRTRANS (Traub, 1976). The empirical method was presented by (Galkin, 1981) that allows to determine magnitudes within the telluric bands with an 3-5% error. Nevertheless, it is still not known if it is possible to obtain a perfect correction of spectrum from telluric lines.

Beforehand, a telluric spectrum should be obtained. Various databases could be used to acquire the Earth's atmosphere spectrum, for example, TAPAS (Transmissions Atmosphériques Personnalisées pour l'AStronomie, or Transmissions of the AtmosPhere for AStromomical data) database (Bertaux, 2014). Telluric spectrum needs to be modified, such that the center of the telluric lines match lines of the object's spectrum. It is easier to calibrate the spectrum by using the strong, deep lines. Since the synthetic telluric's spectra resolution is unbelievably high due to it's origin (it is an idealized model, synthetic spectrum), the telluric spectrum needs to be convolved with a Gaussian and multiplied by a normalization factor in order to lower the spectral resolution. As soon as these steps are done, an object spectrum needs to be divided by the telluric spectrum in order to finally get rid of the telluric lines.

Another method of telluric reduction is to use a telluric standard star, one who's spectrum is featureless and precisely known (for example slow rotating hot stars, A stars or Horizontal Branch stars or white dwarfs) and

use it for cleaning the object of interest spectrum. Such stars usually have signal-to-noise ratio S/N $\geq$ 100. A reduction method based on this idea was discussed by (Vacca, 2003) following almost the same process as (Maiolino, 1996). A-type telluric standard star needs to be observed close to and in the same time when the star of interest is observed. Theoretical model of Vega (the brightest star in the Lyra constellation with a well known spectrum, also an A-type star) spectrum is used to remove intrinsic H lines in the telluric standard star spectrum. In short, construction a telluric correction spectrum is this: normalizing the A star, shifting the Vega spectrum to the determined radial velocity of the A star, scaling and reddening the Vega spectrum to match the A star observed magnitudes, convolving the kernel, constructed from a small region around an absorption feature in the A star and Vega spectra, with the processed model of Vega and scaling the equivalent widths of the different H lines to match the A star lines. The convolved model is then divided by the A star spectrum. Finally, multiplying the result by the observed target spectrum removes the telluric features in the spectra.

One more useful tool for the telluric reduction is a recently developed Molecfit software (Smette, 2015). This software is versatile but data's FITS files need to be managed in a required way to make the program understand it. The GUI interface of this software simplifies work and graphically shows every reduction step.

Method used in this work was a simplified one. I was provided with the telluric spectrum that covers the spectral range of 9000-9500 Å (it is the region of interest, where S I triplet is located) already scaled to match the telluric lines in observed stars spectra same as in the (Skuladottir, 2016) work. Normalized tellurics were subtracted from normalized stars data and returned to normalized scale by adding 1.

Telluric lines were removed with means of the Python code.

3.3 Results

Resolution of the modeled telluric spectrum was reduced to the resolution of the stars spectra by convolution with the Gaussian with σ = 70 and normalizing it (Figure 3.2). This sigma value was used as a good match. Lower sigma values would not be enough to lower the synthetic telluric spectrum resolution to match the stars spectra, higher sigma values would widen telluric lines so much that, they affect regions on the stars spectra during the reduction.

Next, telluric spectra was subtracted from the sky removed normalized star spectra after centering the star spectra around unity (Figure 3.3a, 3.3b, 3.4a, 3.4b). Formula used is: $newpoint = 1 + (centeredstarflux - convolvedtelluricflux)$.

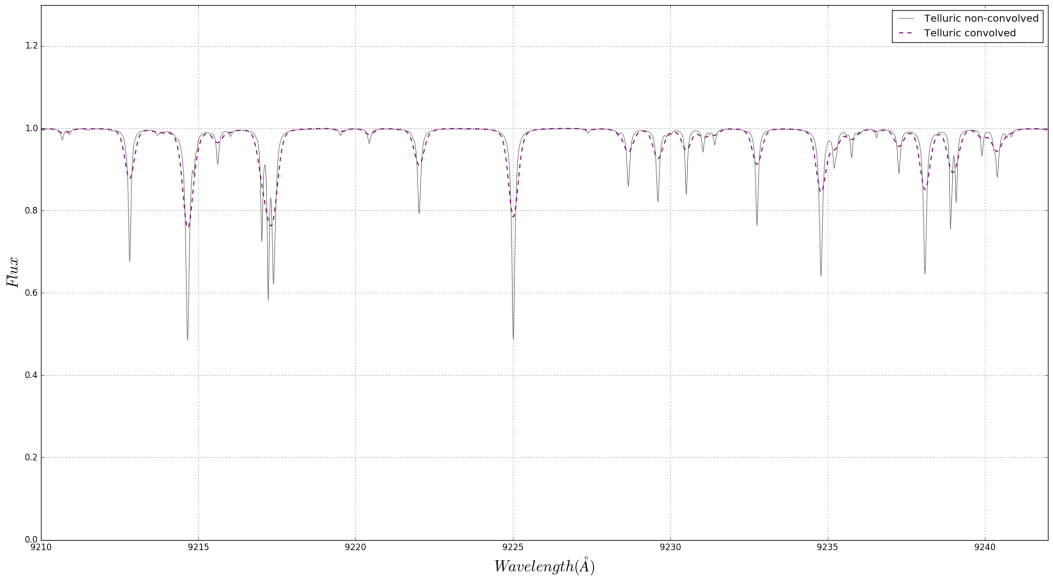

FIGURE 3.2: Telluric convolved with Gaussian (σ=70) is shown as a dotted purple line. Gray line is non-convolved synthetic telluric

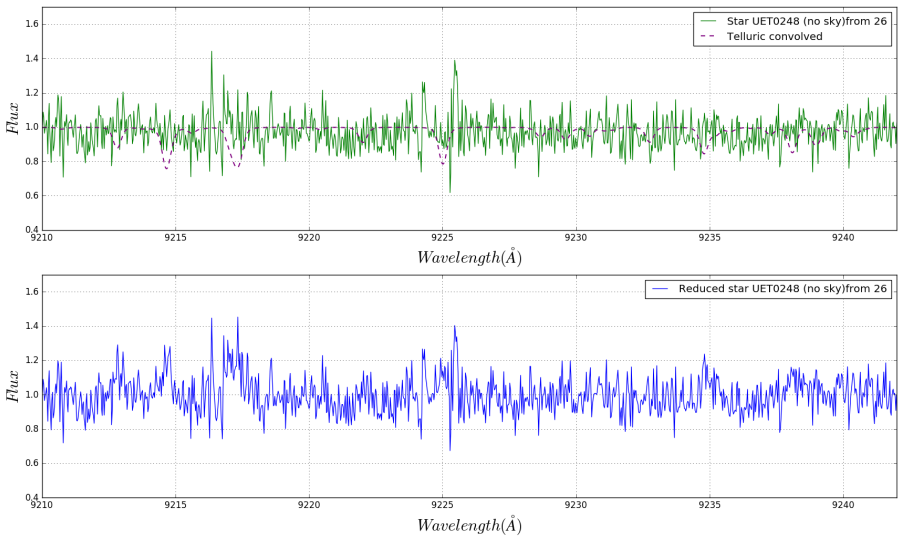

(A)

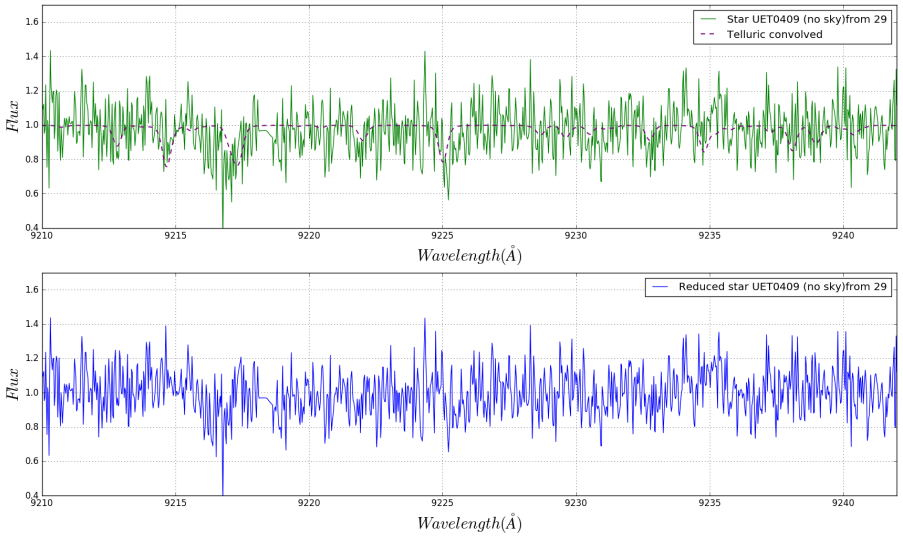

(B)

FIGURE 3.3: UET0248 star sky removed spectra (green) is shown with convolved telluric's spectrum (dotted purple) on the top graph. The star with removed telluric's (blue) is shown on the bottom graph.

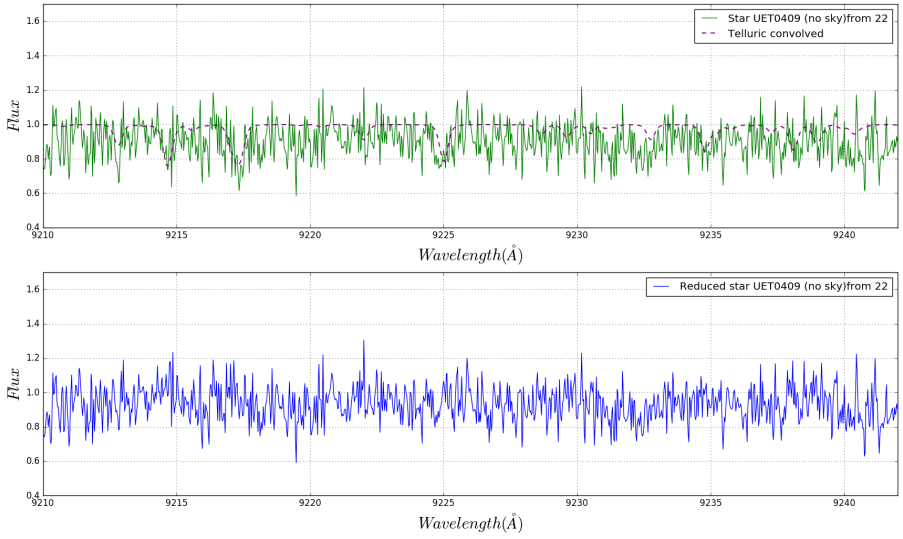

(A)

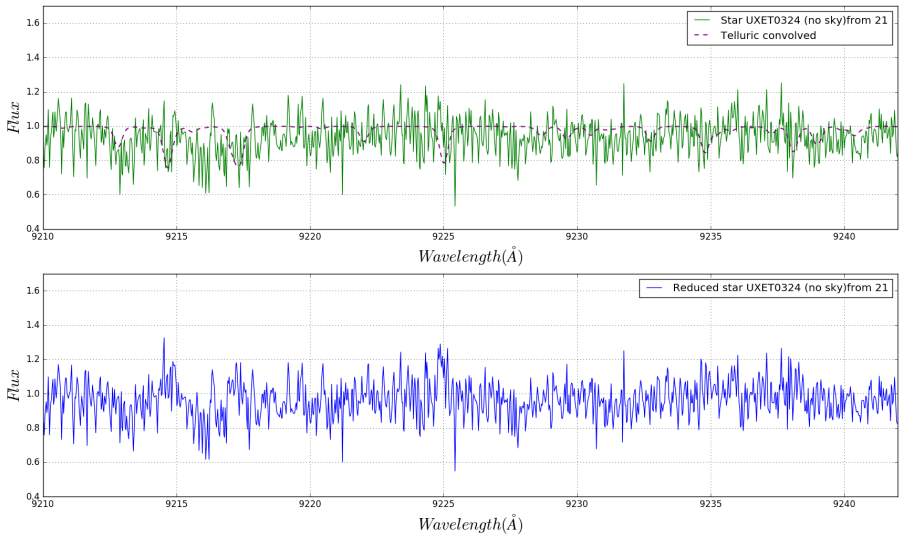

(B)

FIGURE 3.4: Similarly as at Figure 3.3a, 3.3b, but different stars (UET0409 (up) and UXET0324(down).

Chapter 4

Heliocentric corrections and combining spectra

4.1 Heliocentric velocities

After any observations the correct use of reference frame must be taken into account. In this work, data was collected from the Earth that is moving relative to the Sun and the objects of interest are moving relative to Sun. When coordinates are Earth-centered they are called geocentric. For more accurate velocity determination the object's coordinates should be converted to the more convenient reference frame, namely, the Sun reference frame. Sun-centered observations are called heliocentric. The data that is kept in geocentric coordinate frame can make the calculations problematic due to the constant changes of the object velocity relative to the Earth due to the Earth's motion around the Sun (Figure 4.1). Therefore, the most handy coordinate system to keep the data is the heliocentric system.

4.2 Combining spectra

The last step before all individual stars spectra can be analyzed. The spectra that was observed in different times and removed from the sky, the telluric lines and the heliocentrically corrected spectra need to be combined. Faint star spectrum is too uncertain to be totally analyzed from a single observation. Usually, spectra are combined by taking a median in order to increase signal-to-noise ratio and avoid spurious data points that can occur.

Spectra can be median co-added, as follows. All the same stars spectra need to be summed up. In most cases, because of the heliocentric corrections, wavelengths are shifted and this implies that interpolation needs to be done in order to use correct fluxes for the certain wavelengths. As soon as spectra corresponding to the certain wavelengths are summed up, it needs to be normalized, in other words the continuum needs to be set to unity. In the end the summed spectra need to be divided by the total number of spectra.

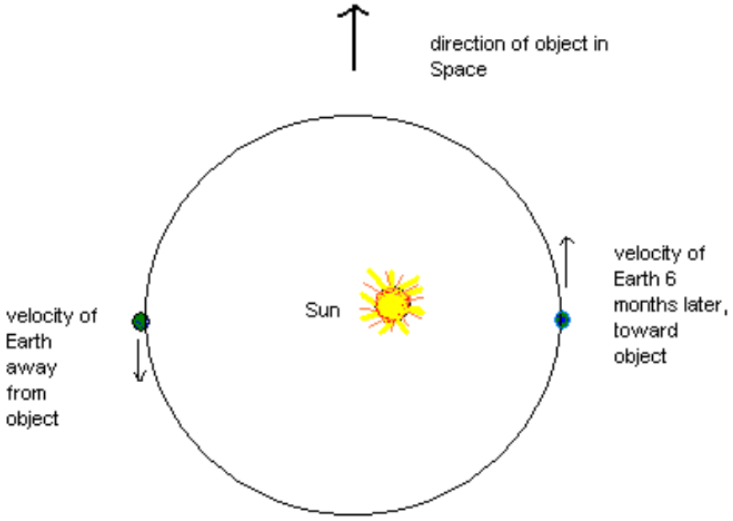

FIGURE 4.1: Earth motion around the sun that produced Doppler Shifts in the object of interest. From (Wood, 2003).

4.3 Results

The Earth rotation around the sun is producing Doppler shifts in the spectrum. The object lines are blue shifted when earth is moving towards the object, and red shifted when it moves away. The Doppler shift formula is Eq.4.1. Here, λ_{new} is the heliocentrically corrected wavelength.

$$\lambda_{new} = \lambda_{old}\sqrt{\frac{1+\frac{v_{helio}}{c}}{1-\frac{v_{helio}}{c}}} \tag{4.1}$$

Once the telluric removal was done, the stars spectra were shifted with respect to the heliocentric velocities. IRAF function "rvcorrect" was used for calculating the heliocentric velocities. Heliocentrically corrected spectrum is shown on the Figure 4.2.

The resulting co-added spectra from one of the stars in the S I triplet region is shown on the Figure 4.3a, 4.3b. Indeed, signal-to-noise ratio is raised and imperfections in the spectra, such as accidentally remaining emission lines and emission lines that are too deep, disappear.

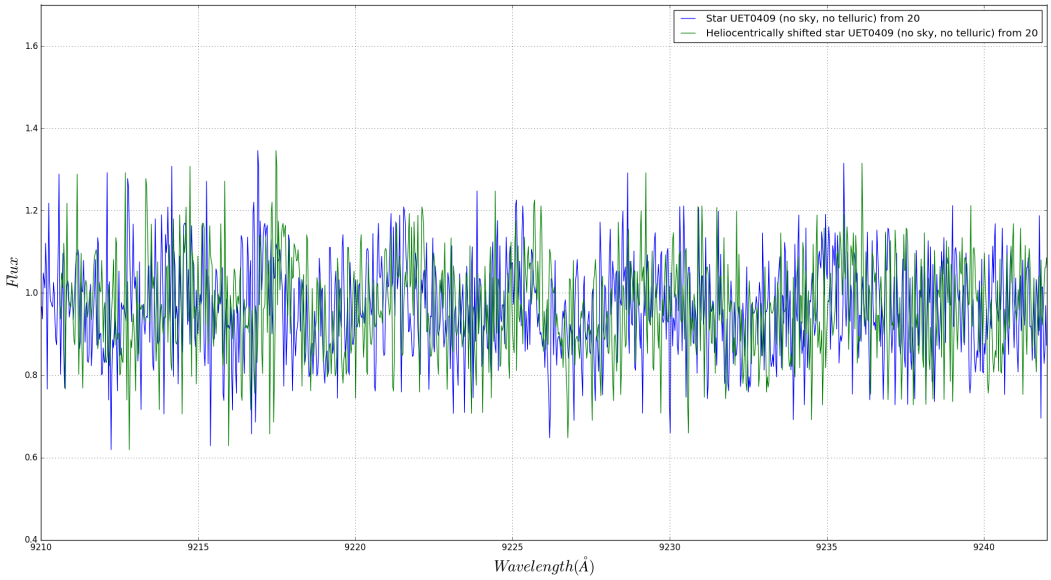

FIGURE 4.2: Heliocentric velocity corrected spectrum of the UET0409 star. Blue - star spectrum, green - heliocentrically corrected star spectrum.

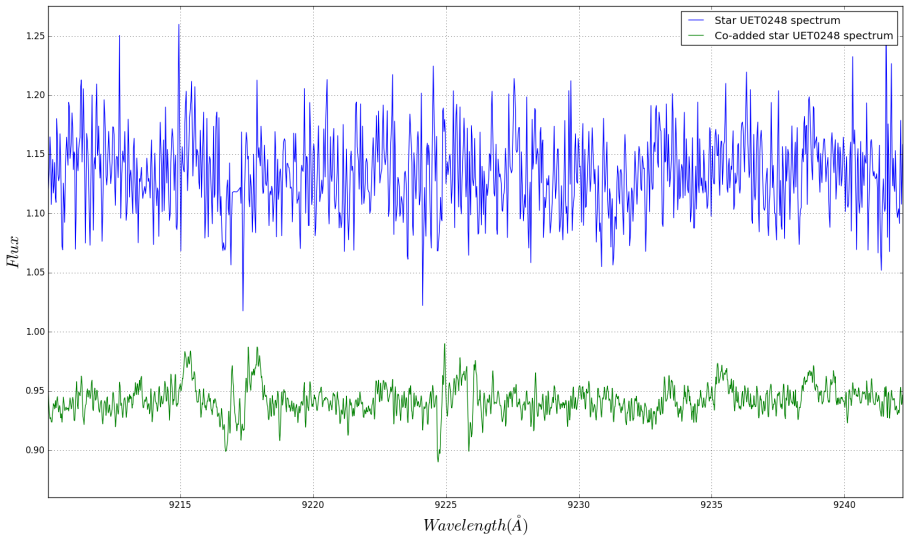

(A)

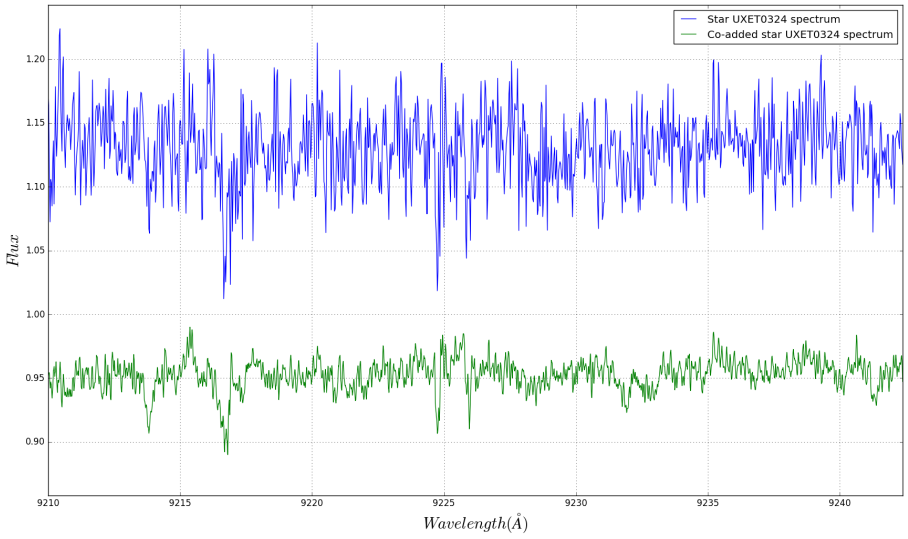

(B)

FIGURE 4.3: Green is co-added star spectrum, blue is not co-added star spectrum. Lines are artificially shifted on the y-axis in convenience sake.

Chapter 5

Results

Before final stars spectra was obtained, several spectra cleaning steps had been taken. First of all, the sky emission lines were deleted, the atmospheric contamination was removed, wavelengths were heliocentrically corrected and the same stars spectra were combined for improving S/N level. The obtained results are compared with the example results from (Skuladottir, 2016) shown on the Figure 5.1.

7 out of 8 stars have spectrum in the S I triplet region. One of the stars, namely UT125 is the telluric star, therefore, it was not analyzed. Thus, 6 stars were analyzed. Figure 5.2a, 5.2b are the resulting spectra of the region of interest (9210-9245Å is shown). The green marked regions show possible sulfur absorption lines location.

In the first green region in all the stars, where the first line from the S I triplet might be, a definite absorption line is seen quite clearly. The central line from the S I triplet is located in the wing of the Paschen ζ line, a bit to the right from the central green region. In comparison with the Paschen ζ line, sulfur line is harder to detect, but it is not seen at all. The last third S I triplet line is the weakest on the Figure 5.1. On our stars the last S I line can't be seen. But, from all the stars spectra the UXET0324 is the star in which sulfur most probably could be found.

It can be concluded since all three S I triplet lines need to be detected in order to claim the sulfur existence on the stars - that there is no conclusive evidence that stars contain sulfur because of the possibility that sky or telluric lines removal went wrong. Surely, an undetected mistake in data reduction could be made, but I believe that the given stars are too faint to be easily analyzed. So, more data samples need to be taken or the stars should not be subjected to analysis until the reliable resolution of the ground-based telescopes is set up.

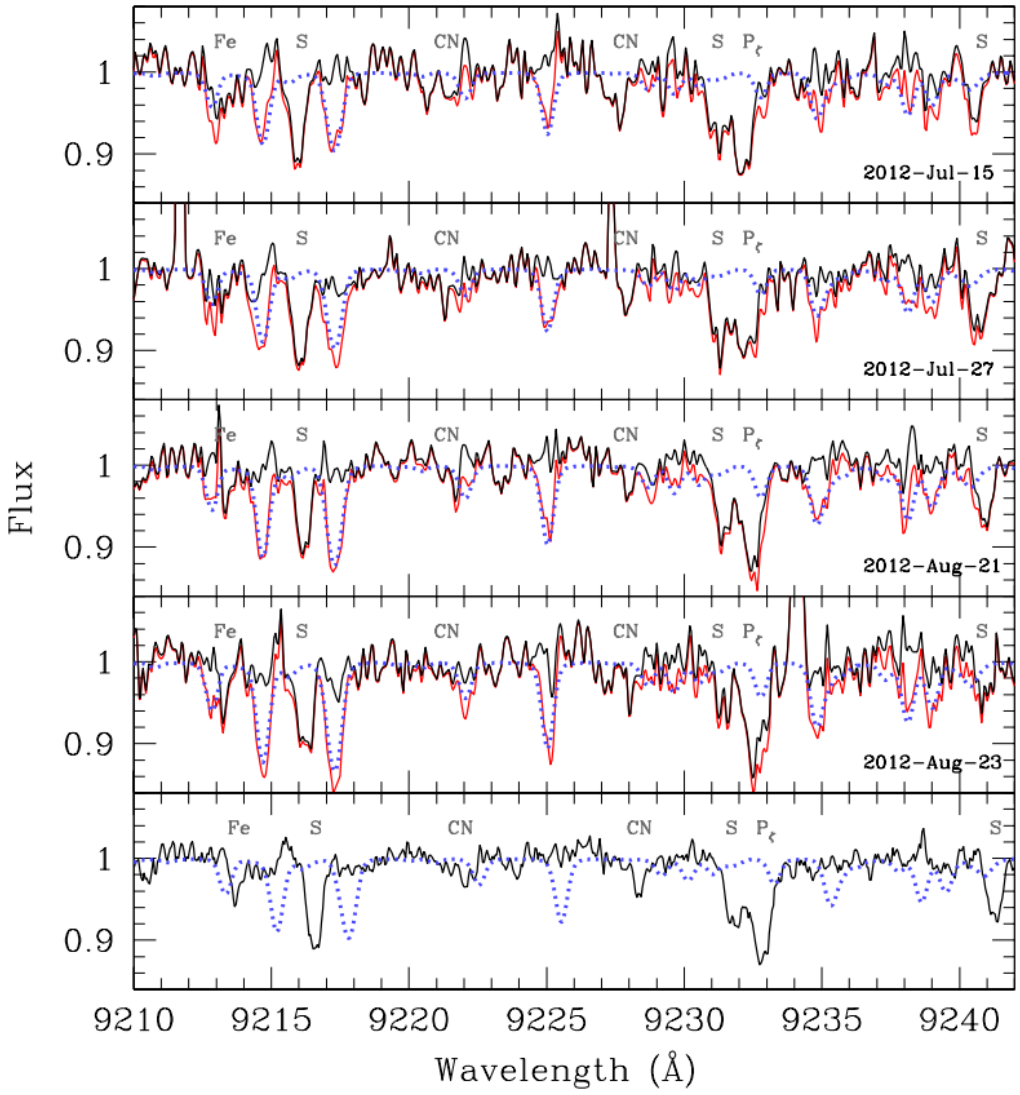

FIGURE 5.1: One of the dSph Sculptor star (ET0048) spectra, in the rest frame of the earth, before (red) and after (black) telluric correction. Blue dotted lines are the synthetic telluric spectra. The final telluric-corrected, co-added spectrum, in the rest frame of the sun is shown on the bottom panel. From (Skuladottir, 2016).

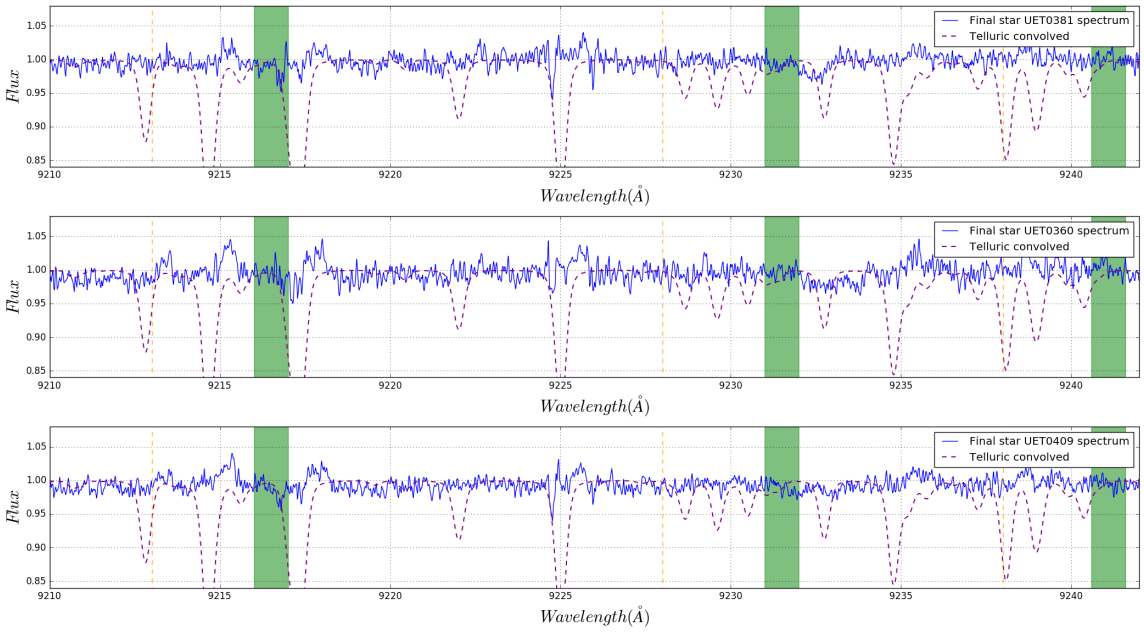

(A)

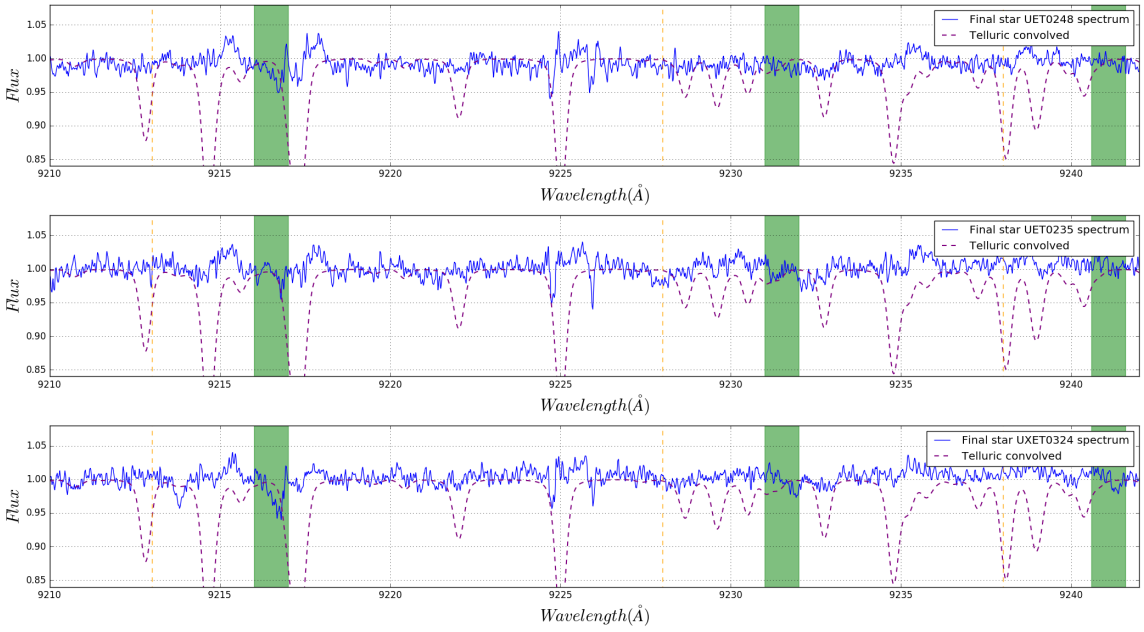

(B)

FIGURE 5.2: Blue lines are the final stars spectra (with no sky radiation, telluric lines, heliocentrically corrected and co-added spectra). Green region are the regions where S I triplet were found on Figure 5.1. Dotted purple lines are telluric's that were removed before spectra were heliocentrically shifted.

Bibliography

Aaronson, M. (1983). "Accurate radial velocities for carbon stars in Draco and Ursa Minor: The first hint of a Dwarf Spheroidal mass-to-light ratio". In: *The Astrophysical Journal* 266, p. 11. URL: https://books.google.nl/books?hl=en&lr=&id=XI59041hwfMC&oi=fnd&pg=PA70&dq=Aaronson+1983,+ApJL,+266,+11&ots=SdsU1tjqUn&sig=0hI5xRLncOF5lpnTHcIRqVN2J2k#v=onepage&q&f=false.

Adelman S. J., Bikmaev I. Gullive A. F. Smalley B. (2002). "Round Table on Instrumentation and Data Processing". In: *AU Symposium, Modelling of Stellar Atmospheres*, p. 13. URL: http://www.astro.keele.ac.uk/~bs/publs/roundtable.pdf.

Battaglia G., Helmi A. Tolstoy E. Irwin M. Hill V. Jablonka-P. (2013). "The kinematic status and mass content of the Sculptor Dwarf Spheroidal Galaxy". In: *The Astrophysical Journal* 2. URL: https://arxiv.org/pdf/0802.4220v2.pdf.

Battaglia G., Tolstoy E. Helmi A. Irwin M. J. Jablonka P.-Hill V. Pasquini L. (2008). "The DART imaging and CaT survey of the Sculptor Dwarf Spheroidal Galaxy". In: URL: http://www.rug.nl/research/portal/files/14452219/c4.pdf.

Bertaux J. L., Lallement R. Ferron S. Boonne C. Bodichon R. (2014). "TAPAS, a web-based service of atmospheric transmission computation for astronomy". In: *Astronomy and Astrophysics* 564, p. 12. URL: http://www.pole-ether.fr/tapas/resources/doc/Bertaux_tapas_2014_aa.pdf.

Boer T. J. L., Tolstoy E. Hill V. Saha A.-Olsen K. Starkenburg E. Lemasle B. Irwin M. J. Battaglia G. de (2012). "The star formation and chemical evolution history of the sculptor dwarf spheroidal galaxy". In: *A&A* 539.765. URL: http://www.aanda.org/articles/aa/pdf/2012/03/aa18378-11.pdf.

Bonifacio P., Hill V. Molaro P. Pasquini L. Di Marcantonio P.-Santin P. (2000). "First results of UVES at VLT: abundances in the Sgr dSph". In: *Astronomy & Astrophysics* 359. URL: http://articles.adsabs.harvard.edu/cgi-bin/nph-iarticle_query?2000A%26A...359..663B&data_type=PDF_HIGH&whole_paper=YES&type=PRINTER&filetype=.pdf.

Bonifacio P., Sbordone L. Marconi G. Pasquini L. Hill V. (2004). "The Sgr dSph hosts a metal-rich population". In: *Astronomy & Astrophysics* 414. URL: http://www.aanda.org/articles/aa/pdf/2004/05/aa3930.pdf.

Brusadin G., Matteucci F. Romano D. (2013). "Modeling the chemical evolution of the Galaxy halo". In: *Astronomy and Astrophysics* 554, p. 10. URL: http://www.aanda.org/articles/aa/pdf/2013/06/aa20884-12.pdf.

Caffau E., Bonifacio P. Faraggiana R. François P. Gratton R. G.-Barbieri M. (2005). "Sulphur abundance in Galactic stars". In: *Astronomy and Astrophysics* 441.2. URL: http://www.aanda.org/articles/aa/pdf/2005/38/aa2905-05.pdf.

Caffau E., Sbordone L. Ludwig H.-G. Bonifacio P. Spite M. (2010). "Sulphur abundances in halo stars from multiplet 3 at 1045 nm". In: *Astronomical Notes* 331. URL: http://onlinelibrary.wiley.com/doi/10.1002/asna.201011353/epdf.

Cochran A. L., Barnes III T. G. (1981). "Spectrophotometry with a self-scanned silicon photodiode array. I - Instrumentation and reductions". In: *Astrophysical Journal Supplement Series* 45. URL: http://adsabs.harvard.edu/full/1981ApJS...45...73C.

Da Costa, G. S. (1984). "The age of the Sculptor dwarf galaxy". In: *Astrophysical Journal* 285, pp. 483–494. URL: http://articles.adsabs.harvard.edu/cgi-bin/nph-iarticle_query?1984ApJ...285..483D&data_type=PDF_HIGH&whole_paper=YES&type=PRINTER&filetype=.pdf.

Faber S. M., Lin D. N. C. (1983). "Is there nonluminous matter in dwarf spheroidal galaxies?" In: *The Astrophysical Journal* 266. URL: http://adsabs.harvard.edu/full/1983ApJ...266L..17F.

Galkin V. D., Arkharov A. A. (1981). "Determination of Extra Atmospheric Monochromatic Stellar Magnitudes in the Region of Telluric Bands". In: *Soviet Astronomy* 25. URL: http://adsabs.harvard.edu/full/1981SvA....25..361G.

Geisler D., Smith V. V. Wallerstein G. Gonzalez G. Charbonnel C. (2001). ""Sculptor-ing" the Galaxy? The Chemical Compositions of Red Giants in the Sculptor Dwarf Spheroidal Galaxy". In: *Astrophysical Journal* 129.3, p. 17. URL: http://iopscience.iop.org/article/10.1086/427540/pdf.

— (2005). ""Sculptor-ing" the Galaxy? The Chemical Compositions of Red Giants in the Sculptor Dwarf Spheroidal Galaxy". In: *Astronomy & Astrophysics* 129.3. URL: http://iopscience.iop.org/article/10.1086/427540/pdf.

Gutiérrez-Moreno A., Moreno H. Cortés G. (1982). "A study of atmospheric extinction at Cerro Tololo Inter-American observatory". In: *Publications of the Astronomical Society of the Pacific* 94. URL: http://www.jstor.org/stable/40678027?seq=1#page_scan_tab_contents.

— (1986). "A study of atmospheric extinction at Cerro Tololo Inter-American observatory. II". In: *Publications of the Astronomical Society of the Pacific* 98. URL: http://iopscience.iop.org/article/10.1086/131923/pdf.

Hammonds, M. (2013). "Andromeda and the 13 Dwarfs". In: *Australian Science*. URL: http://www.australianscience.com.au/space/andromeda-and-the-13-dwarfs/.

Honeycutt R. K., Ramsey L. W. Warren W. H. Ridgway Jr.-S. T. (1977). "Spectrophotometry of cool angular-diameter stars". In: *Astrophysical Journal* 215. URL: http://adsabs.harvard.edu/full/1977ApJ...215..584H.

Jenkins, E. B. (2009). "A unified representation of gas-phase element depletions in the interstellar medium". In: *The Astronomical Journal* 700.

URL: http://iopscience.iop.org/article/10.1088/0004-637X/700/2/1299/pdf.

Khomich V. Y., Semenov A. I. Shefov N. N. (2008). "Airglow as an Indicator of Upper Atmospheric Structure and Dynamics (Berlin: Springer)". In: URL: https://books.google.lv/books?hl=en&lr=&id=vlg64lnz70sC&oi=fnd&pg=PA1&dq=Khomich,+V.+Y.,+Semenov,+A.+I.,+%26+Shefov,+N.+N.+2008,+Airglow+as+an+Indicator+of+Upper+Atmospheric+Structure+and+Dynamics&ots=1n1BtFPW2d&sig=qsX5tPmhwEkdKwNn8N-gSRatZ_c&redir_esc=y#v=onepage&q&f=false.

Kobayashi C., Karakas A. I. Umeda H. (2011). "The evolution of isotope ratios in the Milky Way Galaxy". In: *Monthly Notices of the Royal Astronomical Society* 414. URL: http://mnras.oxfordjournals.org/content/414/4/3231.full.pdf+html.

Kobayashi C., Umeda H. Nomoto K. Tominaga N. Ohkubo T. (2006). "Galactic Chemical Evolution: Carbon through Zinc". In: *The Astrophysical Journal* 653, p. 27. URL: http://iopscience.iop.org/article/10.1086/508914/pdf.

Leinert Ch., Bowyer S. Haikala L.K. Hanner M.S. Hauser M.G. Levasseur-Regourd A.-Ch. Mann I. Mattila K. Reach W.T. Schlosser W. Staude H.J. Toller G.N. Weiland J.L. Weinberg J.L. Witt A.N. (1998). "Synthetic spectrum of the integrated starlight between 3,000 and 10,000 A. I - Method of calculation and results". In: *Astronomy and Astrophysics Supplement Series* 127. URL: http://aas.aanda.org/articles/aas/pdf/1998/01/ds1449.pdf.

Letarte, B. (2007). "Chemical analysis of the Fornax dwarf galaxy". In: *PhD Thesis*.

Levasseur-Regourd, A. C. and R. Dumont (1980). "Absolute photometry of zodiacal light". In: *Astronomy and Astrophysics* 84. URL: http://adsabs.harvard.edu/full/1980A%26A....84..277L.

Lundstrom L., Ardeberg A. Maurice E. Lindgren H. (1991). "A synthetic telluric spectrum in the wavelength region surrounding the D1 and D2 lines of sodium". In: *Astronomy and Astrophysics Supplement Series* 91.2. URL: http://articles.adsabs.harvard.edu/cgi-bin/nph-iarticle_query?1991A%26AS...91..199L&data_type=PDF_HIGH&whole_paper=YES&type=PRINTER&filetype=.pdf.

Maiolino R., Rieke G. H. Rieke M. J. (1996). "Correction of the Atmospheric Transmission in Infrared Spectroscopy". In: *The Astronomical Journal* 111.1. URL: http://adsabs.harvard.edu/full/1996AJ....111..537M.

Manduca A., Bell R. A. (1979). "Atmospheric extinction in the near infrared". In: *The Astronomical Society of the Pacific* 91. URL: http://iopscience.iop.org/article/10.1086/130598/pdf.

Mateo, M. (1998). "Detection of H i Associated with the Sculptor Dwarf Spheroidal Galaxy". In: *Annual Review of Astronomy and Astrophysics* 36, pp. 435–506. URL: http://www.annualreviews.org/doi/pdf/10.1146/annurev.astro.36.1.435.

Matrozis E., Ryde N. Dupree A. K. (2013). "Galactic chemical evolution of sulphur. Sulphur abundances from the [S_I] λ1082 nm line in giants". In:

Astronomy and Astrophysics 559, p. 13. URL: http://www.aanda.org/articles/aa/pdf/2013/11/aa22317-13.pdf.

Mattila, K. (1980). "Synthetic spectrum of the integrated starlight between 3,000 and 10,000 A. I - Method of calculation and results". In: *Astronomy and Astrophysics Supplement Series* 39. URL: http://articles.adsabs.harvard.edu//full/1980A%26AS...39...53M/0000053.000.html.

McConnachie, A. W. (2012). "The Observed Properties of Dwarf Galaxies in and around the Local Group". In: *The Astronomical Journal* 144.1, p. 4. URL: http://iopscience.iop.org/article/10.1088/0004-6256/144/1/4/meta.

McCord T. B., Clark R. N. (1979). "Atmospheric extinction 0.65-2.50 μm above Manua Kea". In: *The Astronomical Society of the Pacific* 91. URL: http://iopscience.iop.org/article/10.1086/130538/pdf.

Monaco L., Bellazzini M. Bonifacio P. Buzzoni A. Ferraro F. R.-Marconi G.-Sbordone L. Zaggia S. (2007). "High-resolution spectroscopy of RGB stars in the Sagittarius streams. I. Radial velocities and chemical abundances". In: *Astronomy and Astrophysics* 464.1. URL: http://www.aanda.org/articles/aa/pdf/2007/10/aa6228-06.pdf.

Monaco L., Bellazzini M. Bonifacio P. Ferraro F. R. Marconi G.-Pancino E.-Sbordone L. Zaggia S. (2005). "The Ital-FLAMES survey of the Sagittarius dwarf spheroidal galaxy. I. Chemical abundances of bright RGB stars". In: *Astronomy and Astrophysics* 441.1. URL: http://www.aanda.org/articles/aa/pdf/2005/37/aa3333-05.pdf.

Monkiewicz J., Mould J. R. Gallagher J. S. III Clarke J. T. Trauger-J. T. Grillmair C. Ballester G. E. Burrows C. J. Crisp D. Evans R. Griffiths R. Hester J. J. Hoessel J. G. Holtzman J. A. Krist J. E. Meadows V. Scowen P. A. Stapelfeldt K. R. Sahai R. Watson A. (1999). "The Age of the Sculptor Dwarf Spheroidal Galaxy from Imaging with WFPC2". In: *The Publications of the Astronomical Society of the Pacific* 111.765, pp. 1392–1397. URL: http://iopscience.iop.org/article/10.1086/316447/pdf.

Nissen P. E., Akerman C. Asplund M. Fabbian D. Kerber F. Käufl H. U. Pettini M. (2007). "Sulphur and zinc abundances in Galactic halo stars revisited". In: *A&A* 469.1. URL: http://www.aanda.org/articles/aa/pdf/2007/25/aa7344-07.pdf.

Noll S., Kausch W. Barden M. Jones A. M. Szyszka C. Kimeswenger S. Vinther J. (2012). "An atmospheric radiation model for Cerro Paranal". In: *Astronomy and Astrophysics* 543, p. 23. URL: http://www.aanda.org/articles/aa/pdf/2012/07/aa19040-12.pdf.

Pasquini L., Avila G. Blecha A. Cacciari C. Cayatte V. Colless M. Damiani F. de Propris R. Dekker H. di Marcantonio P. Farrell T. Gillingham P. Guinouard I. Hammer F. Kaufer A. Hill V. Marteaud M. Modigliani A. Mulas G. North P. (2002). "Installation and commissioning of FLAMES, the VLT Multifibre Facility". In: *The Messenger* 110. URL: http://articles.adsabs.harvard.edu/cgi-bin/nph-iarticle_query?2002Msngr.110....1P&data_type=PDF_HIGH&whole_paper=YES&type=PRINTER&filetype=.pdf.

Patat, F. (2008). "The dancing sky: 6 years of night-sky observations at Cerro Paranal". In: *Astronomy and Astrophysics* 481. URL: http://www.jstor.org/stable/95013?seq=1#page_scan_tab_contents.

Patat F., Moehler S. O'Brien K. Pompei E. Bensby T. Carraro G. de Ugarte Postigo A. Fox A. Gavignaud I. James G. Korhonen H. Ledoux C. Randall S. Sana H. Smoker J. Stefl S. Szeifert T. (2011). "Optical atmospheric extinction over Cerro Paranal". In: *Astronomy and Astrophysics* 527, p. 14. URL: http://www.aanda.org/articles/aa/pdf/2011/03/aa15537-10.pdf.

Pietrzyński G., Gieren W. Szewczyk O. Walker A. Rizzi L. Bresolin F. Kudritzki R. P. Nalewajko K. Storm J. Dall'Ora M. (2008). "The ARAUCARIA project: The distance to the Sculptor dwarf spheroidal galaxy from infrared photometry of RR Lyrae stars". In: *The Astronomical Journal* 135, p. 5. URL: http://iopscience.iop.org/article/10.1088/0004-6256/135/6/1993/pdf.

Rayleigh, F. R. S. (1928). "The Light of the Night Sky: Its Intensity Variations when Analysed by Colour Filter. III". In: *Proceedings of the Royal Society of London. Series A* 119. URL: http://www.jstor.org/stable/95013?seq=1#page_scan_tab_contents.

Ryde N., Jonsson H. Matrozis E. (2014). "Is sulphur a typical α element?" In: *Memorie della Societa Astronomica Italiana* 85. URL: http://sait.oat.ts.astro.it/MmSAI/85/PDF/269.pdf.

Sbordone L., Bonifacio P. Buonanno R. Marconi G. Monaco L. Zaggia S. (2007). "The exotic chemical composition of the Sagittarius dwarf spheroidal galaxy". In: *Astronomy and Astrophysics* 465.3. URL: http://www.aanda.org/articles/aa/pdf/2007/15/aa6385-06.pdf.

Seifahrt A., Käufl H. U. Zängl G. Bean J. L. Richter M. J. Siebenmorgen R. (2010). "Accurate radial velocities for carbon stars in Draco and Ursa Minor: The first hint of a Dwarf Spheroidal mass-to-light ratio". In: *Astronomy and Astrophysics* 524, p. 10. URL: http://www.aanda.org/articles/aa/pdf/2010/16/aa13782-09.pdf.

Shapley, H. (1938). "A Stellar System of a New Type". In: *Harvard College Observatory Bulletin* 908. URL: http://articles.adsabs.harvard.edu/full/1938BHarO.908....1S/0000001.000.html.

Shetrone M. D., Bolte M. Stetson P. B. (1998). "Keck HIRES Abundances in the Dwarf Spheroidal Galaxy Draco". In: *The Astronomical Journal* 115.5. URL: http://iopscience.iop.org/article/10.1086/300341/pdf.

Shetrone M. D., Côté P. Sargent W. L. W. (2001). "Abundance Patterns in the Draco, Sextans, and Ursa Minor Dwarf Spheroidal Galaxies". In: *The Astrophysical Journal* 548.2, p. 17. URL: http://iopscience.iop.org/article/10.1086/319022/pdf.

Shetrone M., Venn K. A. Tolstoy E. Primas F. Hill F. Kaufer A. (2003). "VLT/UVES Abundances in Four Nearby Dwarf Spheroidal Galaxies. I. Nucleosynthesis and Abundance Ratios". In: *Astrophysical Journal* 125.2, p. 23. URL: http://iopscience.iop.org/article/10.1086/345966/pdf.

Skuladottir, A. (2016). "Sulphur, Zink and Carbon in the Sculptor Dwarf Spheroidal Galaxy". In: *PhD Thesis*.

Smecker-Hane T., McWilliam A. (1999). "Ages and Chemical Abundances in Dwarf Spheroidal Galaxies". In: URL: http://arxiv.org/pdf/astro-ph/9910211v1.pdf.

Smette A., Sana H. Noll S. Horst H. Kausch W. Kimeswenger S. Barden M. Szyszka C. Jones A. M. Gallenne A. Vinther J. Ballester P. Taylor J. (2015). "Molecfit: A general tool for telluric absorption correction". In: *Astronomy and Astrophysics* 576.A77, p. 17. URL: http://www.aanda.org/articles/aa/pdf/2015/04/aa23932-14.pdf.

Spite M., Caffau E. Andrievsky S. M. Korotin S. A. Depagne E. Spite F. Bonifacio P. Ludwig H.-G. Cayrel R. François P. Hill V. Plez B. Andersen J. Barbuy B. Beers T. C. Molaro P. Nordström B. Primas F. (2011). "First stars. XIV. Sulfur abundances in extremely metal-poor stars". In: *Astronomy and Astrophysics* 528, p. 8. URL: http://www.aanda.org/articles/aa/pdf/2011/04/aa15926-10.pdf.

Suntzeff N. B., Mateo M. Terndrup D. M. Olszewski E. W. Geisler D. Weller W. .. (1993). "Spectroscopy of Giants in the Sextans Dwarf Spheroidal Galaxy". In: *The Astrophysical Journal* 418. URL: http://adsabs.harvard.edu/full/1993ApJ...418..208S.

Takada-Hidai M., Takeda Y. Sato S. Honda S. Sadakane K. Kawanomoto S. Sargent W. L. W. Lu-L. Barlow T. A. (2002). "Behavior of Sulfur Abundances in Metal-poor Giants and Dwarfs". In: *The Astrophysical Journal* 573, p. 17. URL: http://iopscience.iop.org/article/10.1086/340748/pdf.

Takeda Y., Hashimoto O. Taguchi H. Yoshioka K. Takada-Hidai M. Saito Y. Honda S. (2005). "Non-LTE Line-Formation and Abundances of Sulfur and Zinc in F, G, and K Stars". In: *Astronomical Society of Japan* 57. URL: http://pasj.oxfordjournals.org/content/57/5/751.full.pdf+html.

Takeda Y., Takada-Hidai M. (2011). "Exploring the [S/Fe] Behavior of Metal-Poor Stars with the S I 1.046 μm Lines". In: *Astronomical Society of Japan* 63. URL: http://pasj.oxfordjournals.org/content/63/sp2/S537.full.pdf+html.

Timmes F. X., Woosley S. E. Weaver T. A. (1995). "Galactic Chemical Evolution: Hydrogen Through Zinc". In: *The Astrophysical Journal* 617, p. 114. URL: http://arxiv.org/pdf/astro-ph/9411003v1.pdf.

Tolstoy E., Hill V. Irwin M. Helmi A. Battaglia-G. Letarte B. Venn K. A. Jablonka P. Shetrone-M. Arimoto N. Abel T. Primas F Kaufer A. Szeifert T. Francois P. Sadakane K. (2006). "The Dwarf galaxy Abundances and Radial-velocities Team (DART) Large Programme – A Close Look at Nearby Galaxies". In: *The Messenger* 133. URL: https://www.researchgate.net/profile/F_Primas/publication/252564810_The_Dwarf_galaxy_Abundances_and_Radial-velocities_Team_(DART)_Large_Programme_-_A_Close_Look_at_Nearby_Galaxies/links/0a85e53bd176ed16ed000000.pdf.

Tolstoy E., Hill V. Tosi M. (2009). "Star-Formation Histories, Abundances, and Kinematics of Dwarf Galaxies in the Local Group". In: *Annual Review of Astronomy & Astrophysics* 47.1. URL: http://www.annualreviews.org/doi/pdf/10.1146/annurev-astro-082708-101650.

Tolstoy E., Venn K. A. Shetrone M. Primas F.-Hill V. Kaufer A. Szeifert T. (2003). "VLT/UVES Abundances in Four Nearby Dwarf Spheroidal Galaxies. II. Implications for Understanding Galaxy Evolution". In: *The*

Astrophysical Journal 125.2, p. 17. URL: http://iopscience.iop.org/article/10.1086/345967/pdf.

Traub W. A., Stier M. T. (1976). "Theoretical atmospheric transmission in the mid- and far-infrared at four altitudes". In: *Optical Society of America* 91. URL: https://www.osapublishing.org/ao/abstract.cfm?uri=ao-15-2-364.

Vacca W. D., Cushing M. C. Rayner J. T. (2003). "A Method of Correcting Near-Infrared Spectra for Telluric Absorption". In: *Publications of the Astronomical Society of the Pacific* 115. URL: http://irtfweb.ifa.hawaii.edu/~spex/Telluric.pdf.

Wood, E. (2003). "Telluric Line Removal in Astrophysical Spectroscopy". In: *ASEN/ATOC 5235*, p. 15. URL: http://irina.eas.gatech.edu/ATOC5235_2003/Erin_Wood-paper.pdf.